Characterising the stimulus-response function of mouse C-Low threshold mechanoreceptors to mechanical stimuli *in vivo*

Evangelia Semizoglou[1], Laure Lo Re[2], Steven J. Middleton[3], Jimena Perez-Sanchez[3], Tommaso Tufarelli[4], David L. Bennett[3], Kim I. Chisholm[5]

[1] Department of Neurology, Brigham & Women's Hospital, Harvard Medical School, Boston, USA

[2] Tafalgie Therapeutics, Campus de Luminy, Marseille, France

[3] Nuffield Department of Clinical Neurosciences, University of Oxford, Oxford, UK

[4] School of Mathematical Sciences, The University of Nottingham, Nottingham, UK

[5] School of Life Sciences, The University of Nottingham, Nottingham, UK

Abstract

C-low threshold mechanoreceptors (C-LTMRs) in animals (termed C-tactile (CT) fibres in humans) are a subgroup of C-fibre primary afferents, which innervate hairy skin and respond to low threshold punctate indentations and brush stimuli. These afferents respond to gentle, touch stimuli and are implicated in mediating pleasant/affective touch. These afferents have traditionally been studied using low-throughput, technically challenging approaches, including microneurography in humans and teased fibre electrophysiology in other mammals. Here we suggest a new approach to studying genetically labelled C-LTMRs using *in vivo* calcium imaging. We used an automated rotating brush stimulus and Von Frey filaments, applied to the hairy skin of anaesthetised mice to mirror light and affective touch. Simultaneously we visualised changes in C-LTMR activity and confirmed that these neurons are sensitive to low-threshold punctate mechanical stimuli and brush stimuli with a strong preference for slow brushing speeds. We also reveal that C-LMTRs are directionally sensitive, showing more activity when brushed against the natural orientation of the hair. We present *in vivo* calcium imaging of genetically labelled C-LTMRs as a useful approach that can reveal new aspects of C-LTMR physiology.

Introduction

C-fibres are often studied as the peripheral substrates for painful sensory experiences, including their role in chronic pain. However, it has been known for more than 30 years, that in humans [1] and other mammals[2], [3], [4], [5], [6] this heterogeneous population of afferents also includes a subset which preferentially respond to low-threshold mechanical stimuli, and are thought to drive pleasant touch in humans. This subset of C-fibres, known in humans as C tactile (CT) fibres and in

animals as C-low threshold mechanoreceptors (C-LTMRs) respond to slow and gentle brush stimuli[7], [8], [9], [10], [11] and low force skin indentation [4], [8], [9], [12].

While having first been discovered in cats more than 80 years ago [2], CT-fibres/C-LTMRs have now been well characterized in humans[1], [8] and other mammals [2], [3], [4], [5], [6]. Despite an extended period of study, the methodology used to assess C-LTMR activity and function has remained largely unchanged and technically challenging. Methods including teased fibre recordings in animals and microneurography in humans are labour intensive and very low throughput.

Despite such methods being limited to a small number of specialised groups, our understanding of CT/C-LTMR physiology and their role in the mammalian sensory experience has grown rapidly. We know that both CT fibres in humans and C-LTMRs in many mammals (including non-human primates[5]), can be found in hairy skin, show slow conduction velocities, respond to low force indentation of the skin and show vigorous activity in response to slow brushing stimuli at what is considered a pleasant speed, around 1-10cm/s[7], [8], [9], [10], [11]. Uniquely among mechanoreceptive afferents, increasing stimulus speeds past 10cm/s reduces CT-fibre activity, resulting in an inverted U-shaped tuning curve to brush speed[7]. This stimulus response function is similar in other animals, though shifted to a preference for even slower speeds[10], [13]. This stimulus response function mirrors the reported pleasantness of the brush stimulus, linking CT fibre activity with perceived pleasantness of a given mechanical stimulus[7], [14].

More recently, the study of C-LTMRs has led to a number of discoveries about their gene expression profiles and dependence on ion channels[15], [16]. Several studies have identified molecular markers of rodent C-LTMRs including vGLUT3[12], Tafa4[3], Tyrosine Hydroxylase (TH)[4]. Another population of sensory neurons implicated in pleasurable touch are those that express MRGPRB4 (but not other markers such as TH)[17], [18]. In particular, TH is a marker of a major group of C-LTMRs and makes up ~10% of all dorsal root ganglion (DRG) neurons[4]. TH-positive C-LTMRs innervate mouse hairy skin as longitudinal lanceolate endings surrounding hair follicles[4], [15]. Li et al. showed, using intracellular recordings, that TH-positive DRG neurons function like human C-LTMRs and have low mechanical thresholds, C-fibre range conduction velocities and respond to cooling stimuli[4]. However, studying C-LTMR excitability at single neuron level is challenging, low throughput, and as a result often overlooked.

In this manuscript we discuss a new way to visualize the activity of C-LTMRs, using *in vivo* calcium imaging of the TH-positive C-LTMR population. This technique gives us access to hundreds of DRG neurons simultaneously, facilitating high-throughput assessment of C-LTMRs and their stimulus-response profiles to natural stimuli in a physiologically preserved environment. Using our paradigm,

we show that mouse C-LTMRs respond to punctate and dynamic mechanical stimuli, resembling human CT-fibre afferents. Unexpectedly we identify that C-LTMRs are directionally sensitive to brush stimuli.

Materials and Methods

Animals

All experiments involving mice were performed in accordance with United Kingdom Home Office regulations (Guidance on the Operation of Animals, Scientific Procedures Act) and Laboratory Animal Science Association Guidelines (Guiding Principles on Good Practice for Animal Welfare and Ethical Review Bodies). Experiments were performed in accordance with protocols detailed in a UK Home Office Licence.

All mice were group-housed in individually ventilated cages, with free access to food and water, in humidity and temperature-controlled rooms, with a 12 h light-dark cycle.

$TH^{CreERT2}$[19] mice were sourced from Jackson Labs (Strain #:025614). To label TH-positive cells transgenically we crossed $TH^{CreERT2}$ mice with Cre-dependent a TdTomato reporter line (Ai14, Jax, Strain #:007914) resulting in mice expressing TdTomato in TH-positive neurons (TH-TdTomato). To transgenically express GCaMP in C-LTMRs we crossed the $TH^{CreERT2}$ mice with the RCL-GCaMP6f mouse line (Ai95D, The Jackson, Laboratory, US, Strain #: 024105) to create a mouse in which GCaMP is expressed in TH-positive cells ($TH^{CreERT2}$GCaMP6 mouse). Two adult TH-TdTomato mice were used for immunohistochemistry and ten adult $TH^{CreERT2}$GCaMP6 mice were used for in vivo microscopy.

Tamoxifen injections

TH-TdTomato and $TH^{CreERT2}$GCaMP6 mice received tamoxifen in adulthood. Tamoxifen (Sigma) was dissolved at 20mg/ml in corn oil by sonication for 1hr at 37˚C. Once dissolved the tamoxifen was further diluted to 4mg/ml. Mice received a single IP injection at 50mg/kg and were used for in vivo microscopy or DRG extraction for immunohistochemitry at least 1 week after tamoxifen injection.

Labelling efficiency of TH-positive cells

Pup injections

In 2 TH-TdTomato mice, sensory neurons we labelled through viral transduction. To achieve this, 5µl adeno-associated viral vector, serotype 9 (AAV9) expressing GCaMP6s (AAV9.CAG.GCaMP6s.WPRE.SV40, Addgene, USA) was injected subcutaneously in the nape of the neck of pups (P2-P6), using a 10µl Hamilton syringe. Pups were returned to their home cage. The DRGs were extracted after at least 10 weeks post-injection.

Immunohistochemistry

To assess the efficiency of labelling TH-positive cells through systemic injections in pups, we carefully excised the left L4 DRG in adult mice, washed them in PBS and post-fixed them for 2-3hrs in 4% paraformaldehyde (PFA). After fixation was complete DRGs were cryoprotected in 30% sucrose (0.02% sodium azide) over night. The DRGs were then embedded in Optimal Cutting Temperature (Tissue-Tek) to be frozen and cryosection into 10µm sections before mounting onto glass slides.

The tissue was allowed to dry and was preserved at -80˚C before further processing. To label cells, the tissue was rehydrated and blocked with 10% goat serum (1h). The slices were then incubated overnight at 4˚ with Anti-GFP antibodies (Ab13970, Abcam), diluted 1:1000. Following incubation with primary antibody the slides were washed and incubated with Goat anti-chicken secondary antibody conjugated to Alexa Fluor 488 (A-11039, Invitrogen), diluted 1:1000, for 2 h at room temperature. DAPI-containing media (Fluoromount-G with DAPI, eBioscience) was used to coverslip the tissue. The DRG sections were imaged with a LSM 710 laser-scanning confocal microscope (Zeiss).

Evaluation of transfection efficiency

To assess the transfection efficiency of systemic pup injections of AAV9-GCaMP, 6-10 images were analysed per mouse (n=2). The number of TH-positive cells were counted by an experienced observer and displayed against the number of cells that were TH and GCaMP-positive.

In vivo Ca^{2+} imaging of *C-LMTRs*

At least 1 week after tamoxifen injection, mice were anaesthetized with an initial injection of urethane (12.5% wt/vol) with a dose of 0.3ml (37.5mg urethane). After 15 minutes additional doses were administered depending on reflex activity until surgical depth was achieved (absence of hind limb and corneal reflex activity). Mice were placed on a homeothermically controlled heating mat with a rectal probe to control their body temperature at 37˚C. Their back was shaved, and an incision was made in the skin over the spinal cord at the level of L3-L5. The muscle and connective tissue overlying the vertebrae were carefully removed and a laminectomy was performed which was extended laterally (to the left side) to include exposure of the L4 DRG. Once the DRG was visible the dura and perineurium were left intact but cleaned with sterile normal saline (0.9%) and cotton buds. The exposed DRG was stabilized between a lateral recumbent and prone position, using spinal clamps (Precision Systems and Instrumentation). This positioning ensured a stabilized DRG focusable using an upright microscope. The DRG was covered with silicone elastomer (World Precision Instruments, Ltd) to maintain a physiological environment and to prevent it from drying during imaging.

The anaesthetized and stabilized mouse was then placed under Eclipse Ni-E FN upright confocal/multiphoton microscope (Nikon) and the ambient temperature was locally maintained at 32˚C and the rectal temperature at 37˚C. All timelapse images were recorded through a 10x air objective at an imaging rate of around 4 Hz with an open pinhole. The open pinhole allowed collection of out-of-focus light and as such reduced the effect of biological movements[20]. A 488-nm Argon ion laser line was used to excite GCaMP and a 500–550 nm filter was used for collection.

Brush stimulation

During *in vivo* microscopy the mouse leg was stimulated with a rotating brush stimulator. All mice undergoing in vivo microscopy were stimulated with the rotating brush (n=10). To create a standardized brush stimulus the head of a make-up brush with wide soft bristles (to maximise the stimulation area while minimizing the impact of brush distance: Boots, Lime, Crime Aquarium Brush Set) was attached to a motor (RS Components, RS PRO Brushed Geared motor). The motor was driven by a variable current power source (Hanmatek HM305 bench supply with constant current/voltage output). The relationship between voltage input and brush speed is described in Table 1. The direction of the brush could be reversed by alternating polarity. The speed of 1.55cm/s was the slowest speed reliably achieved. Given that the natural growth orientation of the leg hair in mice is to grow from proximal to distal direction, so that the tip of the hair is pointing towards the paw, the brush was placed such that it would brush from torso to paw (with the hair) and in the reverse direction (against the hair). The brush was allowed to rotate 4 times at every speed before the speed was changed in a random order.

Speed	Voltage
1.55cm/s	1.5V
3cm/s	2.9V
6cm/s	5.8V
10cm/s	9.6V
20cm/s	19.2V
30cm/s	29V

Table 1: relationship between voltage input and brush speed

Von Frey Stimuli

To assess responses to punctate stimuli von Frey filaments with difference bending forces were used to stimulate across 4 locations on the leg each, for a total of 12 stimuli across 12 sites, covering the same stimulation area as the brush stimulus. Nine mice received von Frey stimulation during *in vivo* microscopy. The following filaments were applied in random order: 0.07g, 0.16g and 0.4g.

Time lapse analysis

Time lapse recordings were aligned to a reference frame using the NIS (Nikon Imaging Software) Align Application (Elements AR0.30.01). The resulting stabilized recording was used to extract fluorescence traces over time using Fiji/ImageJ version 2.3.0. The free hand selection tool was used to select regions of interest (ROIs) for each cell. To select out all cell bodies, including from neurons that did not respond to external stimuli, mice were culled under the microscope and the calcium

signal allowed to increase in the cells. An additional ROI for the background was selected over a region with no cell bodies present. The fluorescence intensity of the pixels present in each ROI was averaged for each time frame, resulting in a single fluorescence trace per ROI. The resulting traces were processed further using R version 3.6.1 and RStudio version 1.2.5001: The background trace was subtracted from each cell body ROI at each time frame. The resulting background-subtracted traces were normalized using the following formula:

$$\frac{\Delta F}{F} = \frac{F_t - F_0}{F_0}$$

Where F_t is the fluorescence intensity at time t and F_0 is the averaged fluorescence intensity over a baseline period, prior to the onset of any stimulation (here a 20 second period starting 40 second prior to the first stimulus).

To define responsiveness over a stimulation period an objective threshold was set which would categorize a cell as responding. This was determined against a gold standard (manual selection by an experienced observer – see Supplemental Fig. 1). The threshold was determined by comparing the maximum response in a stimulation period, with the maximum response in a baseline window. Of the thresholds tested, the following was found to be the most accurate: A response is present if:

$$F_{Max} > 1.1(Max\ F_{Bl}) + 5\ (\sigma\ F_{Bl})$$

Where F_{max} is the maximal fluorescence intensity over the stimulation period, $Max\ F_{Bl}$ is the maximum fluorescence intensity over a baseline period (defined relative to each stimulation period, here defined as 5 second starting 10 second before the stimulus) and $\sigma\ F_{Bl}$ is the standard deviation over said baseline period (see Supplemental Fig. 1).

Analysis for repeated brush stimuli

Analysis for the run-off of responses to brush stimuli was performed on responses to the slowest brushing speed (1.5cm/sec) in Wolfram Mathematica (v12.1). Due to slight variations in the onset of each brush stimulus, we had to determine the exact timing of the brush responses for each animal. To do this, the average trace of responding cells (response defined as in “Time Lapse Analysis”) was determined per mouse. From this average trace the location of 4 “brush windows” was determined for each mouse (equivalent to the 4 peaks of neuronal responses to 4 brush stimuli) using the “FindPeaks” function. To optimise peak detection the following parameters were modified: “blurring scale” (σ), “sharpness” (s), “minimum peak value” (t), until 4 peaks were identified in the average trace of each animal (“average peaks” for brevity).

The time window of the 4 average peaks ± 5 seconds was considered the “brush window” of each brush stimulus. Four such windows were determined per mouse per brush direction (4 windows “with the hair” and 4 windows “against the hair”). These windows were used to select the maximum response to each brush stimulus per cell (4 peak responses “with the hair” and 4 peak responses “against the hair” direction).

Maximum responses/peaks were averaged across cells, per animal. Each animal provided one N. Data from “with the hair” was excluded from one mouse as no responding cells could be identified. Data from “against the hair” was excluded from a separate mouse as 4 peaks could not reliably be identified. With excluded data we had a N of 9 for each direction.

Analysis and graphing were conducted using Wolfram Mathematica (version 12.1,) R (version 3.6.1) and R studio (version 1.2.5001) and Microsoft Office Excel (version 2108).

Results

Post-natal injections of AAV9-GCaMP poorly labelled TH-positive sensory neurons

To establish a protocol for labelling TH-positive C-LTMRs with the genetically encoded calcium indicator GCaMP6 we made use of existing labelling protocols for primary afferent neurons[21]. As previously described[21], new-born TH-TdTomato pups (2-6 days post-natal) received subcutaneous injections of adeno-associated virus, subtype 9 (AAV9) expressing GCaMP. Mice were perfused between 8-10 weeks later, and the labelling efficiency of GCaMP in TH-positive cells assessed (Fig 1). This approach did not label sufficient C-LTMR neurons with GCaMP when assessed in adulthood (Fig 1A-B): among 118 TH-tdTomato positive cells observed, only 8 were found to also express GCaMP6 (Fig 1B). To improve the number of GCaMP+ C-LTMRs, we took an alternative approach and crossed

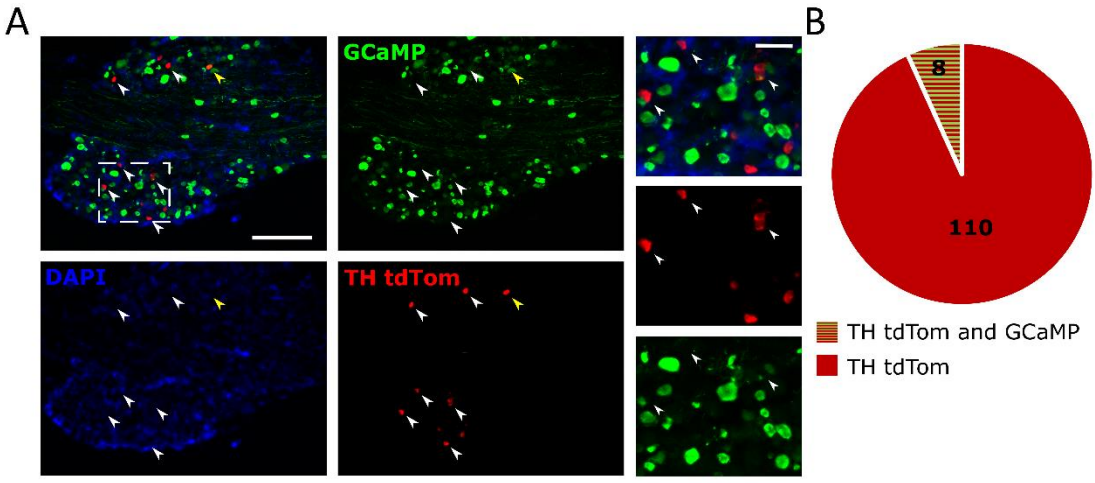

Figure 1: Labelling efficiency of systemic AAV9-GCaMP in TH^{CreERT2}TdTomato mice. A) *Representative images of TH and GCAMP positive cells after systemic injections of AAV9-GCaMP in TH-tdTomato pups. Immunohistochemistry was performed on DRGs excised from adults mice: TH (red), GCaMP (green) and DAPI (blue). White arrow heads indicate examples of TH tdTomato positive cells, yellow arrow heads indicated examples of double positivity (TH tdTomato and GCaMP positivity). Left overview images of whole DRG sections, scale bar = 200µm. Close up inserts (dotted white line) shown on the right, scale bar = 50µm.* ***B)*** *Quantification of A): overlap between TH tdTomato positivity and GCaMP positivity. Proportion of TH tdTomato positive cells is indicated in red (n=2 animals, 110 positive cells), double positivity (TH tdTomato and GCaMP positive cells) is indicated in red and green stripes (n=2 animals, 8 double positive cells).*

the TH^{CreERT2} line with the flox-STOP-*GCaMP6f* line to generate TH ^{CreERT2}GCaMP6 mice, which, following tamoxifen administration, expressed GCaMP selectively in TH-positive neurons/C-LTMRs.

The labelling efficiency was sufficient to visualize a strong GCaMP signal *in vivo*, after exposure and stabilization of the L4 DRG (Fig 2).

To visualize CLTMR activity *in vivo* (Fig 2A) we exposed the L4 DRG in an anaesthetized mouse and visualized the calcium signals using standard single-photon microscopy (confocal microscope with an open pinhole to reduce effects of tissue curvature and biological movement, as described in[20]). An automated rotating brush stimulus (Fig 2B) was used to reproducibly stimulate the ipsilateral leg with low-threshold brush stimulation, as shown in Figure 2. The brush was constructed from a soft make-up brush head (due to its wide and soft bristles), attached to a rotating motor, the speed of which was controlled by a variable current power source. Changes in voltage input altered the brush speed in a direct way (Table 1). The direction of the brush could be reversed by alternating polarity. Von Frey stimuli were applied to the same area as the brush stimulus (Fig 2).

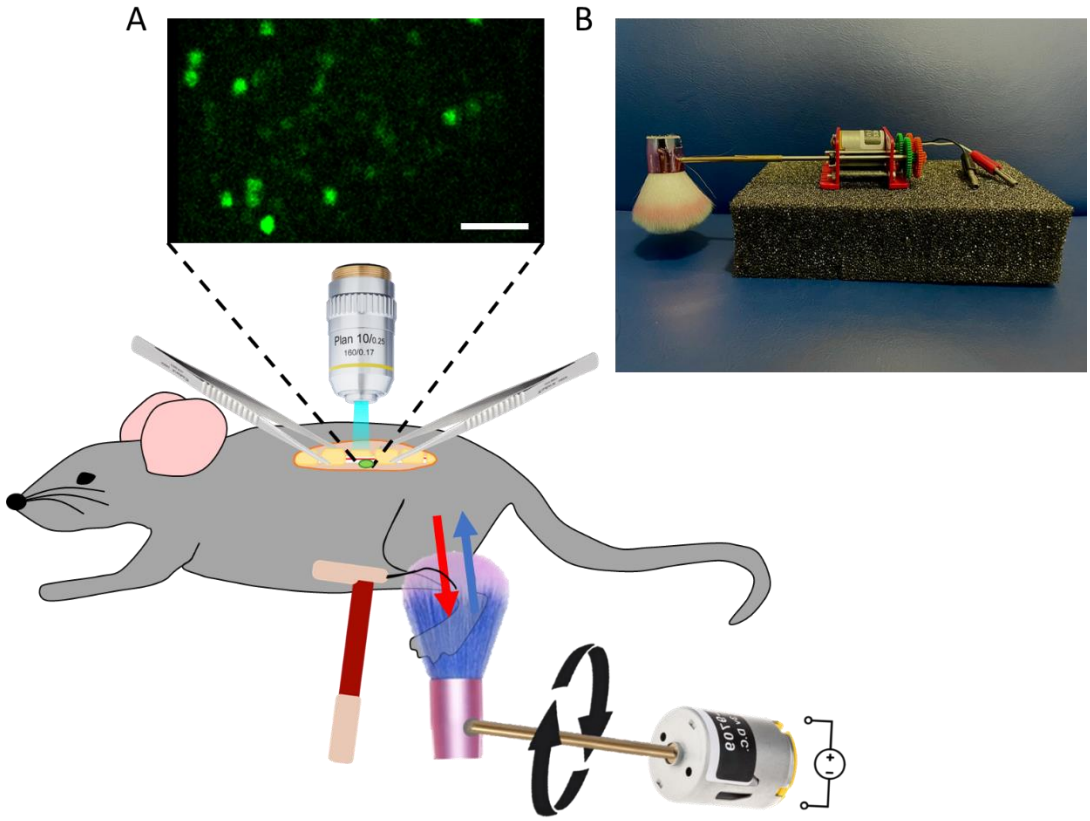

Figure 2: In vivo microscopy set up for DRG imaging. A) *Set-up for in vivo microscopy of L4 DRG. After anaesthesia the L4 DRG is exposed and stabilized through clamps. Standard single photon microscopy is used to visualize neurons in the DRG. During imaging peripheral stimuli are applied*

to the leg of the mouse. To ensure controlled and reproducible brush stimulation a brush head was attached to a rotating motor, which provided control over the speed and direction of the brush stimulus. Red arrow indicates brushing with the hair, blue arrow indicates brushing against the hair. Punctate mechanical stimuli are applied to the same region using Von Frey filaments. ***B)*** *Picture of custom-made rotating brush stimulus.*

TH-positive C-LTMRs respond to brush stimuli in a graded, directionally specific way.

To understand the response profile of mouse C-LTMRs to brush stimuli, a motor-controlled brush stimulus was applied to the ipsilateral leg, and it was sufficient to consistently and reproducibly activate L4 afferents expressing TH (Fig 3). Brushing with the grain of the hair revealed a very strong speed dependent activity pattern in TH-positive neurons, in which slower stimuli preferentially activated TH-positive neurons compared to faster stimuli (Fig 3 A-C), up to 10cm/sec. When the speed is increased to more than 10cm/sec of brushing speed, the relationship between stimulus speed and response intensity is less pronounced, plateauing when brushing with the hair while showing a small peak at 20cm/sec when brushing against the hair (Fig 3 B-C and Movie 1).

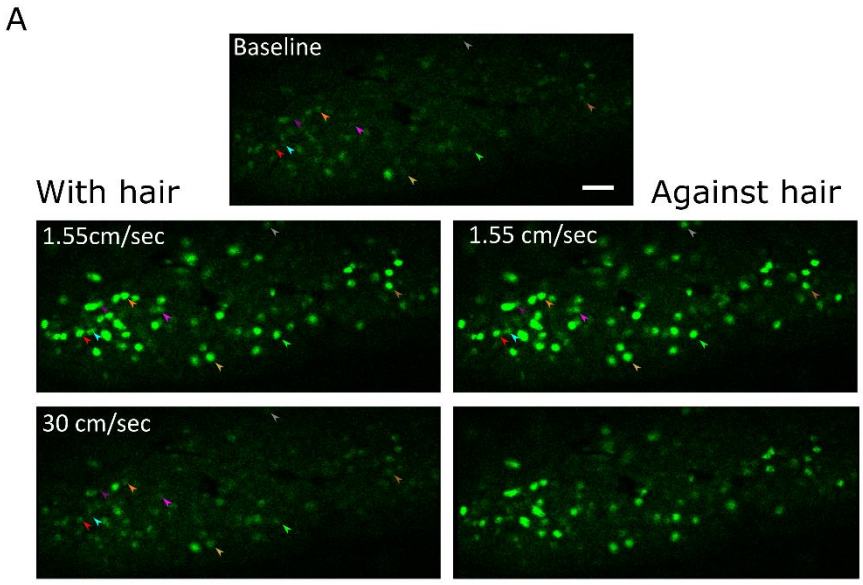

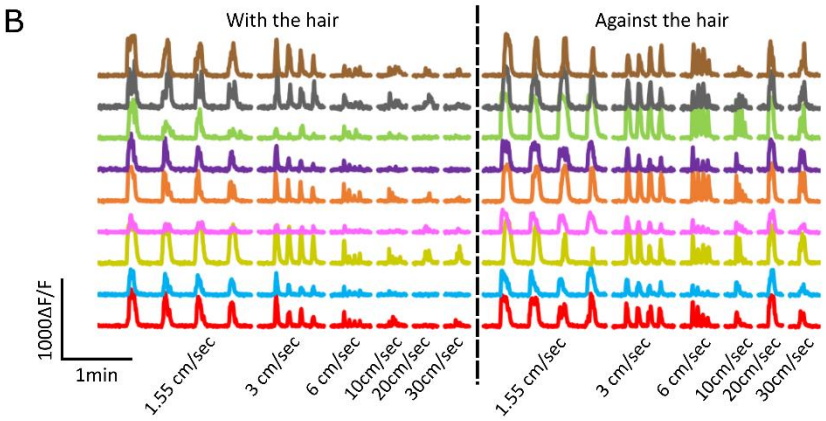

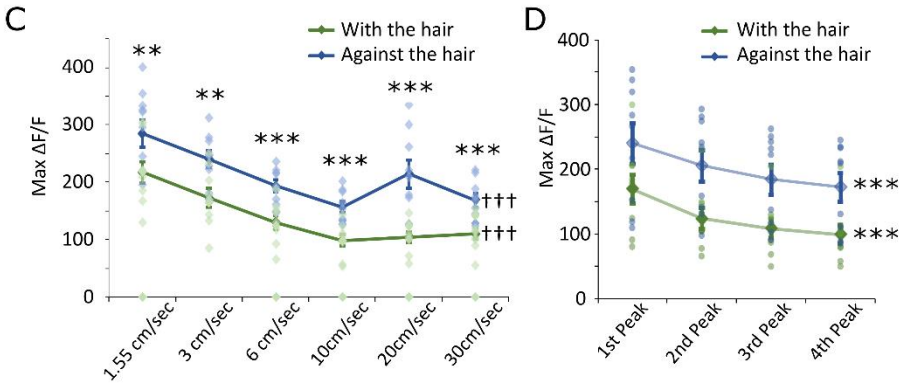

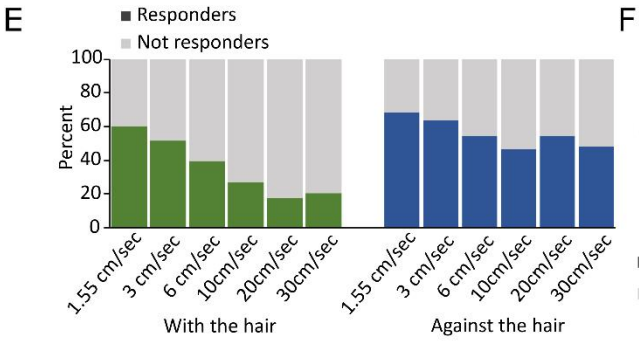

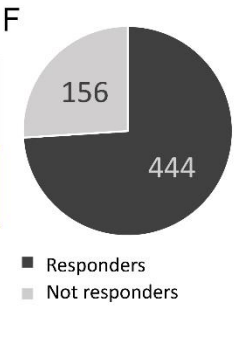

***Figure 3: Speed and directional selectivity of TH-positive cells**. **A)** Representative images of calcium signal from DRGs recorded in vivo during brush stimulation of the ipsilateral leg. Scale bar= 100µm. **B)** Representative traces of TH-positive primary afferents responding to brush stimulation of the ipsilateral leg at different speeds. Each speed was repeated 4 times . **C)** Quantification of calcium signal intensity in cells responding to different speeds of brush. Only responding cells were included and the maximum intensity of the response was averaged across cells. N= 10 mice (total recorded cells = 600). Calcium signal intensity was significantly higher when brushing against the hair at every speed, compared to with the hair: ** p≤0.05, *** p≤0.001. There was a main effect of speed and direction (see text for details): ††† p≤0.001. Data displayed as mean ± SEM. **D)** Quantification of the run-off of neuronal responses during repeated stimulation. Graph showing the maximum intensity (peaks) of neurons during 4 cycles of brush stimulation at 1.5cm/sec. 4 peaks (one at each brush interval) were identified for each cell and averaged per animal. N=9 (one animal data set was removed in the forward direction and one in the reverse direction because peaks could not be reliably detected). There was a significant runoff of responses from 1^{st} to 4^{th} peak as determined by a repeated measures ANOVA: *** p≤0.001 (see text for details). Data displayed as mean ± SEM. **E)** Quantification of the percentage of cells responding to different speeds of brush. N= 10 mice (total recorded cells = 600). **F)** Proportion of cells responding to any brush stimulus. N=10 mice (total recorded cells = 600). See also Movie 1.*

Interestingly, when brushing against the hair the responses of TH-positive cells were enhanced compared to with the hair, at every speed (Fig 3 A-C and Movie 1), with a particularly strong discrepancy at 20cm/sec (Fig 2C). As Mauchly's Test indicates a violation of sphericity the degrees of freedom were corrected using Greenhouse-Geisser estimates of sphericity. There was a significant effect of both speed, $F(2,16) = 65.632$, $p < 0.001$, and direction, $F(1, 8) = 46.4$, $p < 0.001$, with no interaction between direction and speed. The effects size estimated were $\eta^2_p = 0.89$ and $\eta^2_p = 0.85$ respectively. Bonferroni corrected pairwise comparisons between brushing direction at every speed are described in Figure 3 C.

We also observed a reduction in responsiveness (run-down) after repeated rounds of brushing at the very slow speed (Fig 3D). Faster speeds were not assessed because peak detection was most reliable at 1.5cm/sec. The peak intensity of the calcium transients declined from first to fourth brush (each brush was repeated 4 times) both when brushing with the direction of the hair and brushing against the direction of the hair. As Mauchly's Test indicated a violation of sphericity the degrees of freedom were corrected with Greenhouse-Geisser estimates of sphericity. There was a significant decrease in

the peak calcium intensity from 1st to 4th brush stimulus, both in the "with the hair" $F(1.4,11.2) = 43.6$, $p < 0.001$ and "against the hair" direction: $F(1.3, 10.5) = 29.6$, $p < 0.001$. The effect size estimates were $\eta^2_p = 0.85$ and $\eta^2_p = 0.79$ respectively.

A similar relationship was observed in the percentage of cells recruited by each stimulus, with more cells recruited with slower, compared to faster speeds and an overall increased percentage of cells recruited when brushing against the hair, compared to with the hair (Fig 3E).

Overall, we were able to record at least a single response from 74% of recorded cells (Fig 3F), suggesting good recruitment of TH-positive cells in the L4 DRG through brush stimulation of the leg. The total number of cells labelled with GCaMP was detected post-mortem when calcium signals increased inside the cell bodies of cells, revealing all labelled cells.

TH-positive cells respond to punctate stimuli

The response of C-LTMRs to punctate stimuli is still under debate. To address this question we used Von Frey Filaments of different strengths applied at different locations across the leg (covering the same stimulation area as the brush stimulus).

We were able to activate TH-positive cells with punctate stimuli ranging from 0.07 – 0.4g (Fig 4 and Movie 2). While the activation level of TH-positive cells (as measures by peak GCaMP signal) remained stable across stimulation intensities (Fig 4D; $F(2,16)=2.997$, $p=0.078$), higher percentage of responding cells were recruited at higher forces (Fig 4E; Fig $F(2,16)=28.053$, $p < 0.001$).

The Von Frey Stimuli were applied over the same area of the leg as the brush stimuli but covered a reduced area. This reduced area of stimulation (due to the very discrete nature of von Frey stimulation) likely contributes to the relatively low recruitment rate of TH-positive neurons with Von Frey Stimuli (just under 50%, Fig 4F). However, as all receptive fields stimulated with Von Frey stimuli were also stimulated by the brush stimulus we were able to determine the percentage of cells responding to Von Frey stimuli which also responded to brush stimulation; as a measure of specificity to different types of mechanical stimuli (i.e. brush vs punctate stimuli) (Fig 4G). We found that the majority of TH-positive neurons responding to punctate mechanical stimuli also responded to brush stimuli (95%). Additionally, there was no difference in the probability of one type of mechanical stimulation, given another. For example there was no difference in the probability of a response to punctate stimulation (Von Frey at 0.07g, 0.16g and/or 0.4g) in cells responding to brushing with the hair vs against the hair $t(8) = 1.357$, $p = 0.106$ (Supplementary Fig 2a) and there was no difference in the probability of any brush response (with the hair and/or against the hair) given a response to punctate stimulation at 0.07g vs 0.16g vs 0.4g: $F(2, 16) = 0.22$, $p = 0.805$ (Supplementary Fig 2b).

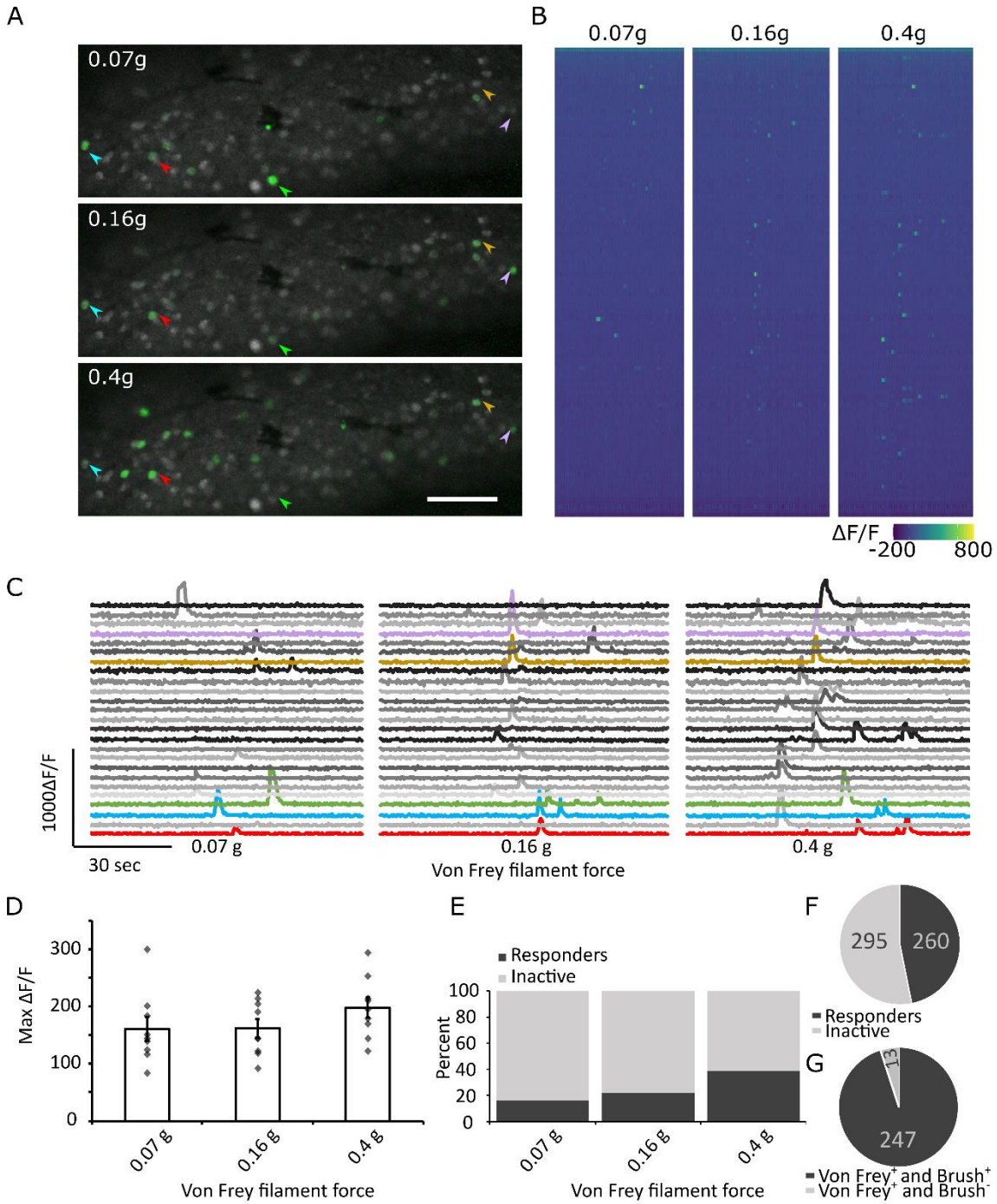

Figure 4: Responses of TH-positive cells to punctate Von Frey stimuli. A) *Representative images of calcium signal from DRGs recorded in vivo during von Frey stimulation of the ipsilateral leg. In green:* $\frac{\Delta F}{F}$ *of standard deviation signal across application of 4 separate Von Frey stimuli on the leg. In grey: standard deviation signal across baseline, to visualize cells that were GCaMP positive but not activated by Von Frey stimulation. Arrows indicate cell bodies that have been activated by Von Frey stimulation. Scale bar= 100µm.* ***B)*** *Heat map of responses in a single mouse DRG during Von Frey stimulation. N = 115 cells.* ***C)*** *Representative traces of TH-positive primary afferents responding to*

Von Frey stimulation of the ipsilateral leg at different forces. Each weight was repeated 4 times at different positions across the leg. Coloured cells represent the same cells as highlighted in ***A*** *with arrows.* ***D)*** *Quantification of calcium signal intensity in cells responding to Von Frey stimulation of different filament forces. Only cells responding were included and the maximum intensity of the response was averaged across cells. N= 9 (total recorded cells = 555).* ***E)*** *Percentage of TH-positive cells responding at different Von Frey filament force strengths. N= 9 (total recorded cells = 555).* ***F)*** *Number of cells responding at least once to a Von Frey stimulus. N= 9 (total recorded cells = 555).* ***G)*** *Number of cells responding to von Frey only (Von Frey^{+} Brush^{-}) vs cells responding to Von Frey and Brush stimuli (Von Frey + Brush +). N=9 animals (total number of cells responding to Von Frey (with or without brush) = 260 cells). See also Movie 2.*

Collectively, we have used targeted genetics combined with *in vivo* calcium imagining to characterise in detail the mechanosensitivity of C-LTMRs innervating the hind leg.

Discussion:

In this manuscript we describe a new approach for the assessment of C-LTMR function by measuring Ca^{2+} flux as a proxy for neuronal activity. We focused on characterising the mechanosensitivity of these afferents, *in vivo,* and believe this approach has the potential to complement more traditional, electrophysiological approaches, providing large-scale data on the activity of multiple C-LTMR sensory neurons simultaneously. This study has been facilitated through the genetic identification of C-LTMRs using the $TH^{CreERT2}$ driver mouse line [4] providing selectively directed GCaMP expression to C-LTMRs. This has allowed us to functionally assess the mechanosensitivity of this specialised sensory subpopulation to punctate and dynamic touch *in vivo*.

A common approach of labelling primary afferents is through the systemic or local injection of AAV particles containing transgenes, such as GCaMP. In particular, intraplantar AAV administration in neonatal mice has been used successfully to target sensory neurons [20], [21]. Our initial strategy was to transduce all sensory neurons using AAV9-GCaMP in mice where C-LTMRs were genetically labelled with a red florescent protein. This method however, was inefficient and unsuccessful in labelling TH-positive C-LTMRs. While the reason remains unclear, another study failed to see C-LTMR infection following intraneural AAV9 and speculated that C-LTMRs may be partially resistant to this serotype[22].

To circumvent this issue, we crossed $TH^{CreERT2}$ mice with the Cre-dependent RCL-GCaMP6 mouse line, which resulted in GCaMP expression only in TH-positive neurons, following tamoxifen injection.

Using this approach, we were successfully able to visualise calcium transients in C-LTMRs in anaesthetised mice. We combined *in vivo* calcium imaging of the exposed DRG with natural stimuli applied to the hairy skin of the ipsilateral leg. These stimuli included automated brush stimulation and low force punctate stimuli. Both stimuli were able to effectively activate C-LTMR neurons in mice and resulted in easily identifiable calcium transients in their cell bodies.

Using this technique, we report sensitivity to low-intensity punctate stimuli with responses to Von Frey stimuli as low as 0.07mN, consistent with the high sensitivity to punctate stimuli reported in rats[6], [12], mice[4], [15] and humans[8], [9].

Intravital microscopy combined with repeated brush stimuli at slow speeds also showed a familiar run down of responses to repeated stimuli. This fatigue is a characteristic feature of C-LTMRs and has been extensively described in humans and experimental animals [1], [10], [23], [24]. In addition, *in vivo* calcium imaging was able to reveal that C-LTMR activity shows the same preference to slower brushing speeds as observed in CT-fibres/C-LTMRS in human[1], [7], [8] and other mammals [3], [25], [26]. However, due to technical constraints, we were unable to stimulate at less than 0.5cm/s – as the motorized brush stimulus was unable to provide consistent results at lower speeds.

This unique relationship between brushing speed and neuronal responses in C-LTMRs has strongly implicated them in the encoding of pleasant touch. Indeed, more than 10 years ago Löken and colleagues found that the inverted U-shaped response curve of CT fibres to increasing brush speed (with preferred brushing velocities around 1-10cm/s) was strongly correlated with the perceived pleasantness of the stimulus[7]. Building on this finding, responses of CT fibres to stroking seem to be modulated by temperature. Brush stimuli at neutral temperatures which are typical of skin temperature, result in preferential activation of CT fibres[14]. These findings, together with patient derived data (suggesting that C-fibres are necessary[27] and sufficient[28], [29], [30] for the detection of pleasant, light touch), were instrumental in associating CT fibre activity with dimensions of affective and social touch [31], [32], [33], [34].

Animal studies similarly reflect the link between C-LTMR activity and positive affect. Stimulation of C-LTMRs resulted in conditioned place preference (CCP), indicative of reward[17], [35]. For example, an intersectional viral chemogenetic approach to stimulate neurons positive for Nav1.8 and $Ca_V3.2$ (an ion channel expressed by and required for normal function of C-LTMRs) was rewarding (as assessed through the CCP paradigm) and promoted touch-seeking behaviours[35]. Conversely, functional deficiency of C-LTMRs (by gene ablation of $Ca_V3.2$) induced social isolation and reduced tactile interactions[35].

Additional associations between C-LTMR activation and reward comes from a population of sensory neurons which appear to be distinct from the TH-positive population. Activation of these MRGPRB4 positive neurons was shown to be rewarding (based on CCP and dopamine release)[17]. MRGPRB4 positive neurons are also reported to respond to brush as determined by *in vivo* Ca^{2+} imaging of their spinal terminal processes but did not respond to punctate mechanical stimuli. It would be interesting in the future to directly compare the stimulus-response function of the TH-positive and the MRGPRB4-positive populations.

Despite this impressive repertoire of findings, associating CT fibres/ C-LTMRs with pleasant/affective touch, it remains difficult to causally link CT fibres/C-LTMR activity to the perception of pleasant touch. In healthy humans the activation of CT fibres necessitates the activation of Aβ fibres, precluding isolated stimulation; and while it is possible to selectively modulate C-LTMR activity in animals, the assessment of the pleasantness of a stimulus is not straightforward.

Using *in vivo* calcium imaging we were able to show that TH-positive cells respond more strongly to brushing stimuli which are applied against the hair as compared to with the hair. Interestingly, in pets with fur, petting/brushing in the direction of hair growth is recommended to avoid stress and discomfort[36], [37], suggesting that brushing against the direction of the hairs is less pleasant. Assuming that such a relationship between grooming direction and pleasantness is seen in our experimental mice, the reported increase in responsiveness of C-LTMRs when brushing against the hair could provide a rare case of dissociation between the pleasantness of a stimulus (against the hair being less pleasant than with the hair) and the activity of TH-positive C-LTMRs (more active when brushing against the hair, compared to with the hair). Indeed, it is likely that to perceive the complex sensory experience of affective touch, direct and unmodulated signalling from a single afferent population is not sufficient. Instead, a combination of sensory signals (peripheral and central) will create the rich experience that is pleasant touch.

There are a number of possible reasons for the observed directional selectivity of C-LTMR responses, including a) a wider excursion of the hair when brushed against its natural orientation, which may cause more prolonged and effective activation of C-LTMRs, b) a possible differential expression of mechanosensitive channels around the hair cell or c) the variation in tension applied to potential protein tethers synthesized by sensory neurons[38]. It should be noted that murine Aδ-LTMRs innervating hairy skin have also been shown to be preferentially tuned to deflection of body hairs in the caudal-to-rostral direction[39] (which would broadly equate to our categorisation of deflection ‘against the hair’). This tuning property is thought to be explained by the finding that Aδ-LTMR lanceolate endings around hair follicles are polarized and concentrated on the caudal side of each

hair follicle[39]. Similarly, Aδ-LTMR directional sensitivity has been shown in rodent glabrous skin, although these afferents appear to be preferentially tuned in the oppositive direction (similar to our 'with the hair' category), while lanceolate endings are polarized in the same way as hairy skin[40]. This suggests that lanceolate ending polarisation may not fully explain LTMR directional sensitivity and other mechanism are likely at play. Indeed, C-LTMR lanceolate endings do not show hair follicle polarisation.

Conclusion

We were able to show that calcium imaging in DRG neurons is a suitable technique to visualise the activity of C-LTMR neurons in anaesthetised mice. We were able to show expected responses to mechanical stimuli, including activation by low-threshold punctate stimuli and preferential responses for slow brushing speeds. We also show an unexpected directional sensitivity of C-LTMRs for brushing against the hair rather than with the hair.

Funding

This work was supported by an Anne McLaren Fellowship, University of Nottingham, held by K.I.C. and funding from the UK Medical Research Council (grant ref. MR/T020113/1), held by D.L.B.

Data Availability Statement

The data and analysis pipelines that support the findings of this study can be made available from the corresponding author [K.I.C.], upon request.

Author contributions

K.I.C., D.L.B. and S. J. M. conceived the project and designed experiments. E.S. and L.L.R. collected the data, K.I.C. and T.T. analysed the data. E.S., L.L.R., S.J.M., J.P.S., T.T., D.L.B. and K.I.C. wrote and edited the manuscript.

Supplementary Figures

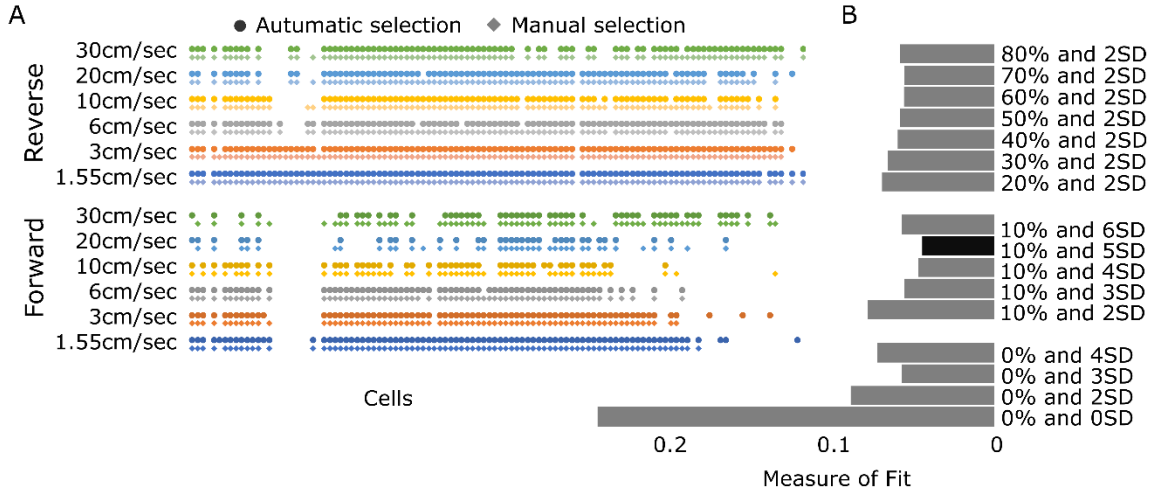

Supplemental Figure 1: Assessment of response threshold. *To assess the validity of a statistical response threshold, the selected responses were compared between different statistical cut offs and manually selected responses, determined by an experienced examiner (gold standard).* ***A)*** *Responses to different types of brush stimuli compared between manual selection (gold standard) and a statistical cut off (in this case a response had to be bigger that 110% of the baseline plus 5 SD of the baseline – see materials and methods for a definition of baseline). Each point represents a response of a cell selected through manual assessment of an experienced researcher. Each diamond represents a response of a cell selected by the statistical cut off procedure. An absence of a point/diamond represents an absence of a response.* ***B)*** *Quantification of the overlap between the gold standard (manual selection) and various statistical cut offs. To quantify the overlap responses were binarized, (as 1 = response or 0 = no response) the value for the manual response was subtracted from the statistical cut off response and the result was squared (to remove negative values). These values were summed and divided by the number of observations. The resulting quantification (measure of fit) ranges from 1 = no overlap between methods, to 0 = perfect overlap between methods. The best automatic threshold tested was baseline + 10% of baseline + 5 SD of baseline. This was used for quantification throughout the manuscript and is highlighted as a black bar in the graph.*

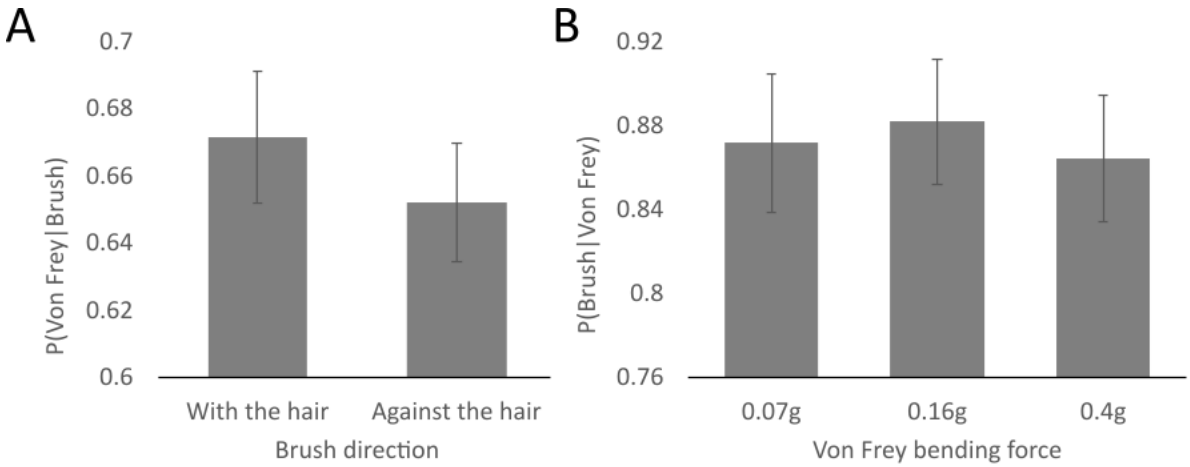

***Supplementary Figure 2: Relationship between responses to punctate and brush stimuli**. **A)** Conditional probability of a response to any punctate mechanical stimuli (Von Frey stimulation of 0.07g, 0.16g and/or 0.4g) given a response to brushing with the hair vs against the hair. **B)** Conditional probability of a response to a brush stimulus (with the hair and/or against the hair), given a response to punctate mechanical stimulation with Von Frey at 0.07g vs 0.16g vs 0.4g.*

Figure legends for supplemental movie

***Movie 1: Speed and directional selectivity of TH-positive cells**: Movie showing the response of TH-positive neurons, labelled with GCaMP to brush stimuli of different speeds (1.55cm/sec, 3cm/sec, 6cm/sec, 10cm/sec, 20cm/sec, 30cm/sec) and directions (with the grain of the hair vs against the grain of the hair). Videos at the top show the raw collected data. Videos at the bottom show the average signal across the whole video (representing most of the recorded and labelled neurons), in grey, and the ΔF/F (see materials and methods section for definition) signal overlayed in green. Scale bar = 100µm.*

***Movie 2: Responses of TH-positive cells to punctate Von Frey stimuli**: Movie showing the response of TH-positive neurons, labelled with GCaMP to Von Frey stimulation of the ipsilateral leg at different forces (0.07gr, 0.16g, 0.4g). Videos on the left show the raw collected data. Videos on the right show the average signal across the whole video (representing most of the recorded and labelled neurons), in grey, and the ΔF/F (see materials and methods section for definition) signal overlayed in green. Scale bar = 100µm.*

References:

[1] M. Nordin, "Low-threshold mechanoreceptive and nociceptive units with unmyelinated (C) fibres in the human supraorbital nerve.," *J Physiol*, vol. 426, no. 1, pp. 229–240, Jul. 1990, doi: 10.1113/jphysiol.1990.sp018135.

[2] Y. Zotterman, "Touch, pain and tickling: an electro-physiological investigation on cutaneous sensory nerves," *J Physiol*, vol. 95, no. 1, pp. 1–28, Feb. 1939, doi: 10.1113/jphysiol.1939.sp003707.

[3] M.-C. Delfini *et al.*, "TAFA4, a Chemokine-like Protein, Modulates Injury-Induced Mechanical and Chemical Pain Hypersensitivity in Mice," *Cell Rep*, vol. 5, no. 2, pp. 378–388, Oct. 2013, doi: 10.1016/j.celrep.2013.09.013.

[4] L. Li *et al.*, "The Functional Organization of Cutaneous Low-Threshold Mechanosensory Neurons," *Cell*, vol. 147, no. 7, pp. 1615–1627, 2011.

[5] T. Kumazawa and E. R. Perl, "Primate cutaneous sensory units with unmyelinated (C) afferent fibers," *J Neurophysiol*, vol. 40, no. 6, pp. 1325–1338, Nov. 1977, doi: 10.1152/jn.1977.40.6.1325.

[6] J. W. Leem, W. D. Willis, and J. M. Chung, "Cutaneous sensory receptors in the rat foot," *J Neurophysiol*, vol. 69, no. 5, pp. 1684–1699, May 1993, doi: 10.1152/jn.1993.69.5.1684.

[7] L. S. Löken, J. Wessberg, I. Morrison, F. McGlone, and H. Olausson, "Coding of pleasant touch by unmyelinated afferents in humans," *Nat Neurosci*, vol. 12, no. 5, pp. 547–548, May 2009, doi: 10.1038/nn.2312.

[8] Å. B. Vallbo, H. Olausson, and J. Wessberg, "Unmyelinated afferents constitute a second system coding tactile stimuli of the human hairy skin," *J Neurophysiol*, vol. 81, no. 6, pp. 2753–2763, 1999, doi: 10.1152/JN.1999.81.6.2753/ASSET/IMAGES/LARGE/9K0690240008.JPEG.

[9] R. H. Watkins *et al.*, "Optimal delineation of single C-tactile and C-nociceptive afferents in humans by latency slowing," *J Neurophysiol*, vol. 117, no. 4, pp. 1608–1614, Apr. 2017, doi: 10.1152/jn.00939.2016.

[10] P. Bessou, P. R. Burgess, E. R. Perl, and C. B. Taylor, "Dynamic properties of mechanoreceptors with unmyelinated (C) fibers.," *J Neurophysiol*, vol. 34, no. 1, pp. 116–131, Jan. 1971, doi: 10.1152/jn.1971.34.1.116.

[11] X. Fang, S. McMullan, S. N. Lawson, and L. Djouhri, "Electrophysiological differences between nociceptive and non-nociceptive dorsal root ganglion neurones in the rat *in vivo*," *J Physiol*, vol. 565, no. 3, pp. 927–943, Jun. 2005, doi: 10.1113/jphysiol.2005.086199.

[12] R. P. Seal *et al.*, "Injury-induced mechanical hypersensitivity requires C-low threshold mechanoreceptors," *Nature*, vol. 462, no. 7273, pp. 651–655, Dec. 2009, doi: 10.1038/nature08505.

[13] R. H. Watkins, "Slow touch in non-human species: translational research into the C-tactile (CT) afferent system," *Curr Opin Behav Sci*, vol. 43, pp. 193–199, Feb. 2022, doi: 10.1016/j.cobeha.2021.10.010.

[14] R. Ackerley, H. Backlund Wasling, J. Liljencrantz, H. Olausson, R. D. Johnson, and J. Wessberg, "Human C-Tactile Afferents Are Tuned to the Temperature of a Skin-Stroking Caress," *The Journal of Neuroscience*, vol. 34, no. 8, pp. 2879–2883, Feb. 2014, doi: 10.1523/JNEUROSCI.2847-13.2014.

[15] S. J. Middleton *et al.*, "Nav1.7 is required for normal C-low threshold mechanoreceptor function in humans and mice," *Brain*, vol. 145, no. 10, pp. 3637–3653, Oct. 2022, doi: 10.1093/brain/awab482.

[16] Y. Zheng, P. Liu, L. Bai, J. S. Trimmer, B. P. Bean, and D. D. Ginty, "Deep Sequencing of Somatosensory Neurons Reveals Molecular Determinants of Intrinsic Physiological Properties.," *Neuron*, vol. 103, no. 4, pp. 598-616.e7, Aug. 2019, doi: 10.1016/j.neuron.2019.05.039.

[17] S. Vrontou, A. M. Wong, K. K. Rau, H. R. Koerber, and D. J. Anderson, "Genetic identification of C fibres that detect massage-like stroking of hairy skin in vivo," *Nature*, vol. 493, no. 7434, pp. 669–673, Jan. 2013, doi: 10.1038/nature11810.

[18] L. J. Elias *et al.*, "Touch neurons underlying dopaminergic pleasurable touch and sexual receptivity," *Cell*, vol. 186, no. 3, pp. 577-590.e16, Feb. 2023, doi: 10.1016/j.cell.2022.12.034.

[19] V. E. Abraira *et al.*, "The Cellular and Synaptic Architecture of the Mechanosensory Dorsal Horn," *Cell*, vol. 168, no. 1–2, pp. 295-310.e19, Jan. 2017, doi: 10.1016/j.cell.2016.12.010.

[20] K. I. Chisholm, N. Khovanov, D. M. Lopes, F. La Russa, and S. B. McMahon, "Large scale in vivo recording of sensory neuron activity with GCaMP6," *eNeuro*, vol. 5, no. 1, pp. 1–14, Jan. 2018, doi: 10.1523/ENEURO.0417-17.2018.

[21] F. Wang *et al.*, "Sensory Afferents Use Different Coding Strategies for Heat and Cold," *Cell Rep*, vol. 23, no. 7, pp. 2001–2013, May 2018, doi: 10.1016/j.celrep.2018.04.065.

[22] Y. A. Bernal Sierra, J. Haseleu, A. Kozlenkov, V. Bégay, and G. R. Lewin, "Genetic Tracing of Cav3.2 T-Type Calcium Channel Expression in the Peripheral Nervous System," *Front Mol Neurosci*, vol. 10, Mar. 2017, doi: 10.3389/fnmol.2017.00070.

[23] A. Iggo and H. H. Kornhuber, "A quantitative study of C-mechanoreceptors in hairy skin of the cat.," *J Physiol*, vol. 271, no. 2, pp. 549–565, Oct. 1977, doi: 10.1113/jphysiol.1977.sp012014.

[24] D. Andrew, "Quantitative characterization of low-threshold mechanoreceptor inputs to lamina I spinoparabrachial neurons in the rat," *J Physiol*, vol. 588, no. 1, pp. 117–124, Jan. 2010, doi: 10.1113/jphysiol.2009.181511.

[25] V. K. Shea and E. R. Perl, "Sensory receptors with unmyelinated (C) fibers innervating the skin of the rabbit's ear," *J Neurophysiol*, vol. 54, no. 3, pp. 491–501, Sep. 1985, doi: 10.1152/jn.1985.54.3.491.

[26] A. François *et al.*, "The Low-Threshold Calcium Channel Cav3.2 Determines Low-Threshold Mechanoreceptor Function," *Cell Rep*, vol. 10, no. 3, pp. 370–382, Jan. 2015, doi: 10.1016/j.celrep.2014.12.042.

[27] I. Morrison *et al.*, "Reduced C-afferent fibre density affects perceived pleasantness and empathy for touch," *Brain*, vol. 134, no. 4, pp. 1116–1126, Apr. 2011, doi: 10.1093/brain/awr011.

[28] H. Olausson *et al.*, "Functional role of unmyelinated tactile afferents in human hairy skin: Sympathetic response and perceptual localization," *Exp Brain Res*, vol. 184, no. 1, pp. 135–140, Jan. 2008, doi: 10.1007/S00221-007-1175-X/TABLES/2.

[29] J. Cole *et al.*, "Unmyelinated tactile afferents underpin detection of low-force monofilaments," *Muscle Nerve*, vol. 34, no. 1, pp. 105–107, Jul. 2006, doi: 10.1002/MUS.20534.

[30] H. Olausson *et al.*, "Unmyelinated tactile afferents signal touch and project to insular cortex," *Nature Neuroscience 2002 5:9*, vol. 5, no. 9, pp. 900–904, Jul. 2002, doi: 10.1038/nn896.

[31] F. McGlone, J. Wessberg, and H. Olausson, "Discriminative and Affective Touch: Sensing and Feeling," *Neuron*, vol. 82, no. 4, pp. 737–755, May 2014, doi: 10.1016/J.NEURON.2014.05.001.

[32] H. Olausson, J. Wessberg, I. Morrison, F. McGlone, and Å. Vallbo, "The neurophysiology of unmyelinated tactile afferents," *Neurosci Biobehav Rev*, vol. 34, no. 2, pp. 185–191, Feb. 2010, doi: 10.1016/J.NEUBIOREV.2008.09.011.

[33] I. Morrison, L. S. Löken, and H. Olausson, "The skin as a social organ," *Exp Brain Res*, vol. 204, no. 3, pp. 305–314, Jul. 2010, doi: 10.1007/s00221-009-2007-y.

[34] J. Liljencrantz and H. Olausson, "Tactile C fibers and their contributions to pleasant sensations and to tactile allodynia," *Front Behav Neurosci*, vol. 8, Mar. 2014, doi: 10.3389/fnbeh.2014.00037.

[35] D. Huzard *et al.*, "The impact of C-tactile low-threshold mechanoreceptors on affective touch and social interactions in mice," *Sci Adv*, vol. 8, no. 26, Jul. 2022, doi: 10.1126/sciadv.abo7566.

[36] M. E. Herron and T. Shreyer, "The Pet-friendly Veterinary Practice," *Veterinary Clinics of North America: Small Animal Practice*, vol. 44, no. 3, pp. 451–481, May 2014, doi: 10.1016/j.cvsm.2014.01.010.

[37] M. L. Casalia, M. A. Howard, and S. C. Baraban, "Persistent seizure control in epileptic mice transplanted with gamma-aminobutyric acid progenitors," *Ann Neurol*, vol. 82, no. 4, pp. 530–542, Oct. 2017, doi: 10.1002/ana.25021.

[38] J. Hu, L.-Y. Chiang, M. Koch, and G. R. Lewin, "Evidence for a protein tether involved in somatic touch," *EMBO J*, vol. 29, no. 4, pp. 855–867, Feb. 2010, doi: 10.1038/emboj.2009.398.

[39] M. Rutlin *et al.*, "The Cellular and Molecular Basis of Direction Selectivity of Aδ-LTMRs," *Cell*, vol. 159, no. 7, pp. 1640–1651, Dec. 2014, doi: 10.1016/j.cell.2014.11.038.

[40] J. Walcher *et al.*, "Specialized mechanoreceptor systems in rodent glabrous skin," *J Physiol*, vol. 596, no. 20, pp. 4995–5016, Oct. 2018, doi: 10.1113/JP276608.